#### Research Article

Ruihao Zhang, Shan Qing\*, Xiaohui Zhang\*, Zhumei Luo, and Yiqing Liu

# Investigation of different nanoparticles properties on the thermal conductivity and viscosity of nanofluids by molecular dynamics simulation

 $\boldsymbol{A}$ 

https://doi.org/10.1515/ntrev-2022-0562 received February 22, 2023; accepted May 19, 2023

Abstract: The mechanisms of thermal conductivity enhancement and the factors influencing viscosity are of great interest in the study of nanofluids, while molecular dynamics (MD) simulations considering nanofluids provide more accurate predictions of microscopic properties than conventional experimental studies. MD simulations of nonequilibrium molecular dynamics and reversing perturbation non-equilibrium molecular dynamics methods were used to study thermal conductivity and viscosity, taking into account a variety of influencing factors, as well as nanoparticle material and volume fraction. Through the analysis of the number density distribution, radial distribution function (RDF), and mean square displacement (MSD), the influences of different nanoparticles (Ag, Cu, Au, and Fe) were described and investigated: Ag particles contribute to 47.0% increase in thermal conductivity of 2.5 vol% nanofluids; Au particles improved the viscosity of 2.5 vol% nanofluids by 20.2%; the number density distribution showed positive linear relationship with the atomic mass; the results of MSD and RDF (mean square displacement and radial distribution function) in combination indicated a positive effect of interfacial nanolayer. The results of this research provide important perspectives for comprehending the impacts of multiple nanoparticles on the micro-thermal properties of nanofluids and also highlight the simulation potential of Au-Ar nanofluids.

the cross-sectional area perpendicular to the

#### **Nomenclature**

heat flux direction (m<sup>2</sup>) heat flow density (J m/s) the length of the *X* direction (m) the length of the Y direction (m) Lennard-Jones L-J MSD R(t) mean square displacement non-equilibrium molecular dynamics **NEMD** Ν number of particles stress tensor (Pa) **RDF** g(r) radial distribution function **RNEMD** reverse non-equilibrium molecular dynamics the molecular spacing between particle i and

particle j (m)  $v_i$  velocity of atom i (m/s) V the volume of the system (m<sup>3</sup>)

# **Greek symbols**

 $\varepsilon$  the energy constant (eV)  $\sigma$  the length constant (Å)  $\eta$  shear viscosity (Pa s) k thermal conductivity (W/m K)

 $\Delta t$  time step (s) T temperature (K)

# \* Corresponding author: Shan Qing, Faculty of Metallurgical and Energy Engineering, Kunming University of Science and Technology, Kunming 650093, China, e-mail: m15087088903@163.com

e-mail: xiaohui.zhang@kust.edu.cn

Ruihao Zhang, Zhumei Luo, Yiqing Liu: Faculty of Metallurgical and Energy Engineering, Kunming University of Science and Technology, Kunming 650093, China

# **Subscripts**

f base fluid

*i* numbering of atom *i* 

j numbering of atom j

nf nanofluids

**Keywords:** molecular dynamics simulation, different nanoparticles, interfacial nanolayer

<sup>\*</sup> Corresponding author: Xiaohui Zhang, Faculty of Metallurgical and Energy Engineering, Kunming University of Science and Technology, Kunming 650093, China,

2 — Ruihao Zhang et al. DE GRUYTER

## 1 Introduction

Being defined as liquid colloidal solutions containing nano-sized solid particles suspended in the base fluid, nanofluids have been widely investigated by researchers on account of their remarkable thermophysical properties and countless potential applications [1,2]. Similarly, as excellent heat transfer media, its high heat transfer capacity and potential applications have been widely applied as heat exchange of devices and energy systems [3,4].

The viscosity of a nanofluids becomes as significant as its thermal conductivity due to the fluids typically involved in the applications mentioned above, as well as drawing a great deal of research attention [5]. Based on molecular dynamics (MD) simulations, these two properties have been investigated and discussed extensively. After comparing the thermal conductivity values between various nanoparticle shapes, Bhanushali et al. [6] concluded that nanowire-shape particles reduce the detrimental impact of surface mechanical resistance on thermal transfer because of their higher aspect ratio. Analogously, nanoparticles with large aspect ratios enhance thermal conductivity with increased heat transfer rates during nanoparticle collisions, a conclusion noted by Ghosh et al. [7] in their study. Zhou et al. [8] demonstrated a comparison of the heat transfer behaviors of Cu-Ar nanofluids by constructing a non-equilibrium molecular dynamics (NEMD) simulation model. The thermal conductivity simulations and their fraction calculations were also presented to explore the relationship between the energy transfer terms of molecular motion and the agglomeration state of nanoparticles. Liao et al. [9] also calculated the potential effects of different initial aggregation structures on the thermal conductivity of various volume fractions using the Cu-Ar nanofluids model, which revealed the microscopic mechanism of the influence on thermal conductivity by nanoparticle structure. Lou and Yang [10] investigated various factors affecting the shear viscosity of Al<sub>2</sub>O<sub>3</sub> water-based nanofluids, namely, particle size, concentration, and temperature through a combination of MD simulations and experiments. Similarly, Jabbari et al. [11] contrasted the functions of particle volume fraction and nanofluids temperature by exploring physical phenomena of SWCNT/water nanofluids employing Green-Kubo MD simulations, which indicated that the volume fraction was the most direct factor of viscosity increase. Zeroual et al. [12] investigated the factors related to the influence of the viscosity of Cu-Ar nanofluids and confirmed that the appearance of compact nanolayers at the boundary between the nanoparticles and the base fluid proved

to be the origin of the influence of the volume fraction over the viscosity.

The presence of nanolayers around nanoparticles, as extensively demonstrated in previous studies above, is an essential factor that relates to the improved thermal conductivity by means of the intermediate thermal resistance that exists among the liquid and solid phases [13,14], also, it is a recognized mechanism for thermal conductivity enhancement and viscosity increase [15]. Akiner et al. [16] simulated the heat transport in Cu-H<sub>2</sub>O systems employing individual copper particles in their study, and the results can be explained brilliantly by interfacial dynamics. Guo and Zhao [17] examined the interfacial layer adsorption properties around the surface of Cu nanoparticles and discovered that the particle-fluid interfacial layer with thickness significantly depending on the nanoparticle diameter was formed around the nanoparticles, which might be exploited to explain the variation in the thermal conductivity. Importantly, the effects of various characteristics of nanoparticles in terms of type, media, and volume density on thermal conductivity were investigated systematically by Cui et al. [18] and the enhancement of thermal conductivity by Ag nanoparticles was better than Cu, Au, and Fe.

In another report by Cui *et al.* [19], a study was conducted for the liquid-solid interfacial absorption layer in nanofluids that had been proven to exist, at the same time, the impacts of different elements on the microstructure were concluded. The abovementioned simulation studies on nanofluids contain different kinds of particles, and several scholars have considered multiple nanoparticle cases, but the combination of thermal conductivity and viscosity studies is insufficient, besides the microscopic laws of different nanoparticles have not been further investigated.

In this study, NEMD based on NEMD and reversing perturbation non-equilibrium molecular dynamics (RNEMD) methods will be used to perform the detailed MD simulations and the main objective is to reveal the mechanisms and comparisons in the thermal conductivity and viscosity strengthening of four types of nanofluids containing different kinds of nanoparticles. In order to evaluate the credibility of the simulations model, the results are presented in comparison with a series of theoretical and experimental data published previously. In addition, the microstructures of nanofluids are explored by the number density study method to further understand the microscopic mechanisms of nanofluids. The number density distribution, mean square displacement (MSD), and radial distribution function (RDF) of atoms in nanofluids containing different types of metal atoms are interpreted systematically.

# 2 Simulation methodology

# 2.1 Choices of potential energy function and parameters

In this research, simulations were established for pure Ar and Cu/Au/Ag/Fe-Ar nanofluids, so as to say that the nanofluid systems were formed by adding structures of four types of nanoparticles in Ar liquid. Although Ar liquid is not a real fluid, this fluid type requires less computational time compared to other complex base fluids such as water, more importantly, its interatomic potential shows the same behavior as the actual base fluid, which facilitates the extension of theoretical models to practical experiments [20]. All simulations were performed by the LAMMPS package (partial use of GPU acceleration) [21,22] and the atomistic visualizations were observed using the technique of Ovito [23].

The interatomic potentials between all the argon atoms are modeled by the 12-6 Lennard-Jones potential, which allows direct use in calculating the interactions of Ar/Ar and Cu/Au/Ag/Fe-Ar in nanofluid systems [24] and enables to improve the speed and computational accuracy of LAMMPS runs with the aid of the latest GPU acceleration capabilities [22]. The mathematical expression is given below.

$$\varphi(r_{ij}) = 4\varepsilon \left[ \left( \frac{\sigma}{r_{ij}} \right)^{12} - \left( \frac{\sigma}{r_{ij}} \right)^{6} \right] \quad (r < r_{c}). \tag{1}$$

The Lorentz Berthelot mixing rules [25] are applied for computing the forces between various atoms.

$$\varepsilon_{\text{Cu/Au-Ar}} = \sqrt{\varepsilon_{\text{Cu/Au}} \times \varepsilon_{\text{Ar}}},$$
 (2)

$$\sigma_{\text{Cu/Au-Ar}} = \left[ \frac{\sigma_{\text{Cu/Au}} + \sigma_{\text{Ar}}}{2} \right], \tag{3}$$

where  $\varepsilon$  denotes the energy constant,  $\sigma$  represents the length constant,  $r_{ii}$  denotes the separation between iwith j particles, and  $r_c$  expresses the cutoff radius  $(\varphi(r_{ij}) = 0 \text{ for } r \ge r_c)$ , typically  $r_c > 2.5\sigma$ , and in this research,  $r_c = 11 \,\text{Å}$ . The energy interactions among different atoms are presented in Table 1 [19].

# 2.2 Heat flux calculation and thermal conductivity formula

One of the prominent properties of nanofluids is thermal conductivity, and the method used to calculate thermal conductivity is predicated on NEMD [26]. This approach

Table 1: L-J potential energy parameters for Cu/Au/Ag/Fe/Ar interactions

Atom pair	$\varepsilon$ (eV)	<b>σ</b> (Å)
Ar–Ar	0.0104	3.405
Cu-Cu	0.4096	2.338
Au-Au	0.4447	2.637
Au-Ar	0.0680	3.021
Cu-Ar	0.0650	2.871
Ag-Ag	0.3447	2.644
Ag–Ar	0.0598	3.025
Fe-Fe	0.5300	2.321
Fe-Ar	0.0740	2.863

supposes that the transport direction occurs along the specific axis (the transport heat flow is set in the x-axis), while the macroscopic behavior of the heat transfer phenomenon is characterized by Fourier's law [27]. In this approach, a temperature gradient needs to be established for a suitable time period first, from which the system attains a steady state [28]. Afterwards, the uniformly varying temperature gradient of the system is measured based on the obtained data, then the thermal conductivity k of the system expressed is as follows:

$$k = -\frac{J}{A \times \nabla T},\tag{4}$$

where  $\nabla T$  is the temperature gradient value, A denotes the area of system cross section orientated perpendicular to heat flow conduction, the value of negative reflects the direction of the temperature gradient, and I suggests the heat flow density value.

The temperature gradient  $\nabla T$  is obtainable on the basis of the formula given below.

$$\nabla T = \frac{\partial T}{\partial x},\tag{5}$$

where x denotes the translation in the direction of heat conduction, and *T* denotes the temperature.

Concretely, the speed-heavy criterion NEMD method presented by Ikeshoji and Hafskjold [29] is applied in this part of the study rationally, while the most important heat flow density *J* is set up using the "Fix Ehex" command.

For a given  $\Delta t$ , J is calculated using the following equation:

$$J = \frac{\Delta \epsilon}{2\Delta t}.$$
 (6)

Dividing by two for the whole system avoids double counting of the heat outflow and inflow directions, which is due to the fact that the system is governed by a periodic boundary condition A, so that  $\Delta t$  denotes a time step.  $\Delta \in$  represents the variation in the incremental atomic energy from the heat source. Figure 1 displays the fluxes from both sides of the heat source, which will be explained in detail during the following validation section.

#### 2.3 Stress tensors and viscosity

The physical quantity that measures the internal friction that impedes the flow of a fluid is called viscosity of a fluid [11]. The analysis of fluid transport properties and thermal properties in MD research relies on the calculation of viscosity, and the calculation of system viscosity is essential in the field of nanofluids research [12].

The calculation of shear viscosity used in this section is based on RNEMD, namely, the MP method [30,31]. The gradient of  $v_x$  is instituted in the *Z*-direction by clipping the liquid as shown in Figure 2, resulting in the X momentum flows along the *Z*-direction, generating a flux of momentum  $j_z(p_x)$  traveling across the *xy*-plane of area A. In other words, the MP method calculates

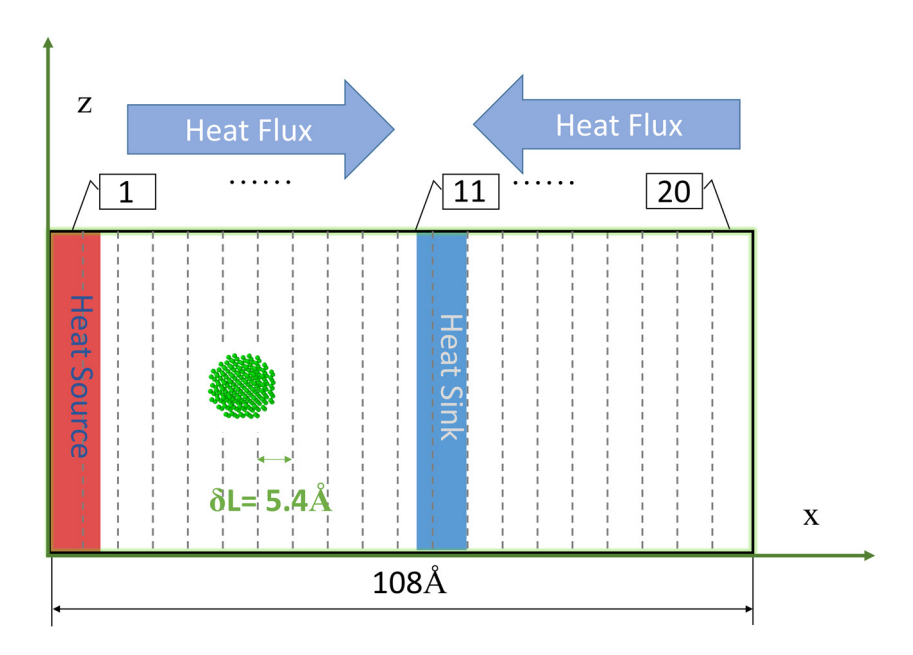


Figure 1: The distribution of the heat source (red) and heat sink (blue) along the x-axis in the simulated nanofluids.

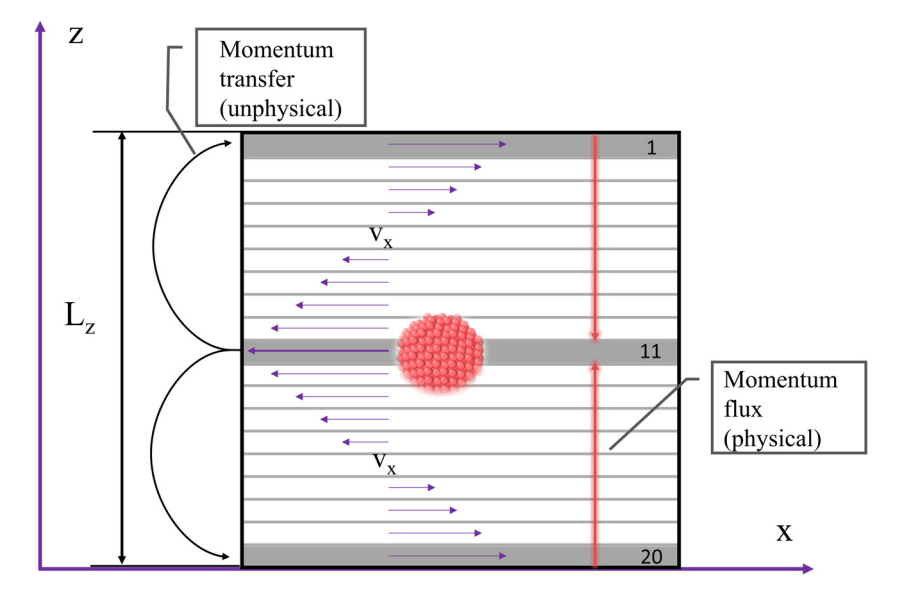


Figure 2: Geometry of the non-equilibrium in the simulated nanofluids.

viscosity by constructing a shear field and combining it with a transverse linear momentum flux [30]. Specifically, the momentum flux  $j_z(p_x)$  represents the x component of the momentum  $p_x$  transmitted along the interface parallel to the direction of flux Z with area A  $(A = L_x L_y)$  in a time period t, as shown by the following formula [31]:

$$j_z(p_x) = -\eta \frac{\partial v_x}{\partial z},\tag{7}$$

where  $\eta$  is the shear viscosity,  $\partial v_x/\partial z$  represents the gradient of the speed in the X-direction over the Z-direction. In order to simplify the understanding and calculation, Eq. (7) is transformed to obtain Eq. (8), which is the formula used in LAMMPS to calculate shear viscosity. In the present research, we divided the momentum in the Z-direction into 20 parts,  $P_{x,1}$  and  $P_{x,11}$  represented the momentum values of part 1 and part 11, respectively. In metal units, the unit of the viscosity is Pas.

$$\eta = -\frac{\sum (P_{x,1} - P_{x,11})}{2\Delta t L_x L_y \left[\frac{\partial v_x}{\partial Z}\right]}.$$
 (8)

#### 2.4 Calculation of RDF

The RDF method is typically used to provide insight into the atomic interactions between two similar or different species [32], where g(r) denotes the probability of discovering adjacent atoms at a specified distance from the central atom. In the present study, the following formula is used for the purpose of exploring the microstructural features of nanofluids [33]:

$$g(r) = \frac{V}{n_a n_b} \left\langle \sum_{i=1}^{n_a} \frac{n_{ib}(r, \Delta r)}{4\pi r^2 \Delta r} \right\rangle, \tag{9}$$

where  $n_a$  and  $n_b$  stand for the amounts of particles;  $n_{ib}$  (r,  $\Delta r$ ) represents the total number of particles within the effective radius (r to  $\Delta r$ ) of the specified particle b; and V indicates the capacity of the system.

#### 2.5 Calculation of MSD

The MSD analysis technique allows for a specific study of nanofluid dynamics properties and also infers reinforced heat transfer principle by nanofluids [34] by the following formula:

$$MSD = R(t) = \langle |\overrightarrow{r_i}(t) - \overrightarrow{r_i}(0)|^2 \rangle, \tag{10}$$

where  $\overrightarrow{r_i}(t) - \overrightarrow{r_i}(0)$  stands for the range vector of the motion at time t of the particle in question, and  $\vec{r}_i(t)$ stands for the parameter space of the particle *i* at moment t. In order to better understand the thermal properties of liquids with nanofluids associated with MSD, the diffusion coefficient (D) is computed at long time intervals according to Einstein's equation as below [35].

$$D = \frac{1}{6} \lim_{t \to \infty} \frac{\mathrm{d}}{\mathrm{d}t} \langle |\overrightarrow{r_i}(t) - \overrightarrow{r_i}(0)|^2 \rangle. \tag{11}$$

# 3 Validation of the MD simulation model

## 3.1 Thermal conductivity

In the present simulation calculations, a simulation box of 108 Å  $\times$  55 Å  $\times$  55 Å (x, y, and z directions) was structured, and the absorbed energy value of the system was determined by applying the "Fix Ehex" command to the heat source and the heat sink. Before simulating the Cu/Au/Ag/Fe-Ar nanofluids, an effective calculation of the thermal conductivity of pure Ar was performed at 85 K to verify the accuracy of the simulation [35], with the power value of the process set to 0.05 eV/ps (with the metal units in LAMMPS). First of all, the entire simulation system (the box of 7,039 pure Ar atoms) was equilibrated for 0.8 ns to obtain a consistent temperature of 85 K in the regular system synthesis (constant volume and temperature, NVT), which used the Nose-Hoover thermostat with 2 fs time steps. Subsequently, the NEMD running in the microcanonical ensemble (constant energy and volume, NVE) was employed to calculate the thermal conductivity.

During the temperature equilibrium relaxation, 20 layers with the thickness of  $\delta L = 5.4 \,\text{Å}$  in the X-direction were set up. The heat source and heat sink regions were set up near the first and eleventh layers, respectively, which allowed the simulated heat flow to be transported uniformly in the x-axis direction for up to 54 Å. As shown in Figure 3, the temperature variation in the 20 layers has been monitored, and the temperature gradient of each region approached a V-shaped line segment when they reached 600,000 steps, indicating that the overall simulated system has reached a well-balanced NEMD simulations. Finally, the computed thermal conductivity turned out to be 0.1298, which has an error of 0.006% compared

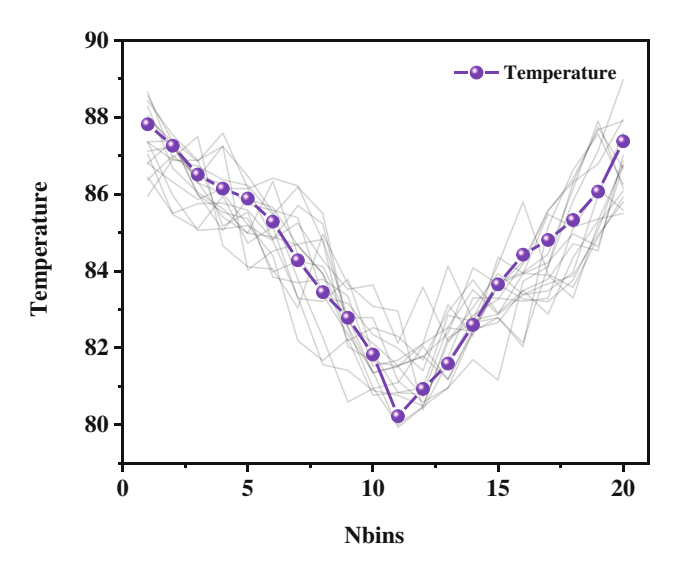


Figure 3: The temperature gradient of the 20 layers in the simulation box.

to the announced 0.1290 [9], indicating that the system established is stable and reliable.

In Figure 4, The Cu–Ar nanofluids simulation results from this study are employed for verification with previous studies, and the similarity of the simulation results is indicated by the similar fold lines and data points [9,28,36,37]. The phenomenon of steady increment of the heat conductivity with volume fraction, as well as the reciprocal proximity of the simulation results, indicates that the established system has excellent simulation value.

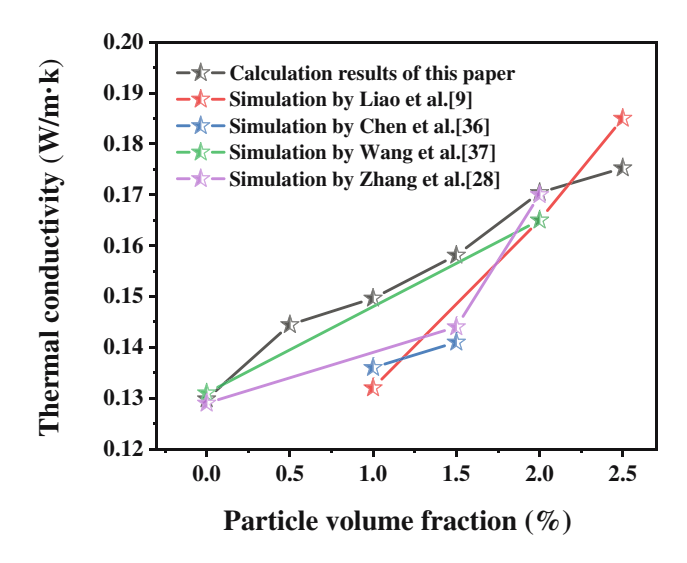


Figure 4: Comparison of thermal conductivity between MD simulation results for Cu-Ar nanofluids.

#### 3.2 Viscosity

In this study, a faster and easier MP method than the Green-Kubo method was applied, and the use of interatomic potential and the application of the RNEMD method were validated gradually [30,31]. Compared with the NEMD method for calculating thermal conductivity, in the MP method, the system has been separated into 20 bins according to the Z-direction (any coordinate direction is possible), and the velocity gradient was constructed by exchanging the momentum components in the *Z*-direction of atoms in bins 1, 20, and 11, and then forming a shear field, while exchanging and counting the momentum exchange in the *Z*-direction for calculation (Figure 2). Among them, the choice of the momentum exchange frequency Nhas a certain influence on the results of the system viscosity calculation, and after several calculations of the linearity in the velocity gradient, N = 5 was selected in this study.

In this section, the system was warmed to 94.4 K using NPT ensemble in order to guarantee the presence of a stable liquid argon phase, where the time step  $\Delta t = 2$  fs and cutoff radius  $r_c = 13$  Å. The ensemble NVT was sufficient to bring the system to balance state after being equilibrated for 50,000 steps. Similar to the NEMD method, the uniformly distributed speed distribution (Figure 5) was got for 0.4 ns under the canonical ensemble NVT (constant volume and temperature), which indicated that a stable velocity gradient was obtained in the *X* direction, and the final reliable viscosity results were obtained by applying Eq. (8).

The system was generated by creating argon atoms arranged into a simulation box of 55 Å  $\times$  55 Å  $\times$  55 Å (4,000 pure Ar atoms), and the final result was 2.78  $\times$  10<sup>-4</sup> Pa s.

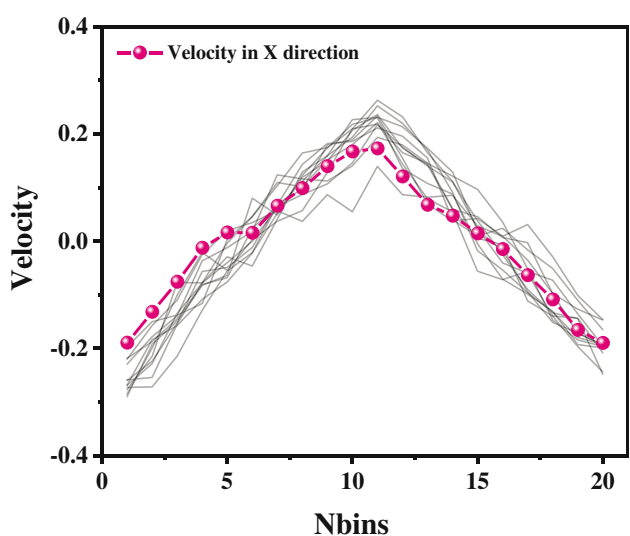


Figure 5: The viscosity gradient of the 20 layers in the X-direction.

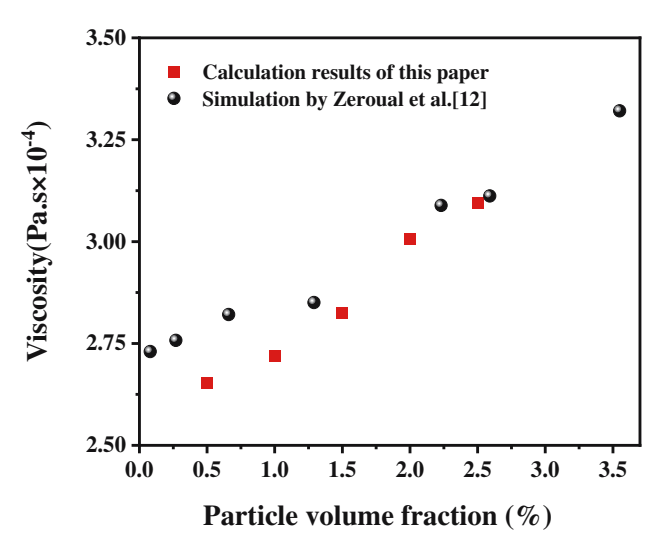


Figure 6: Comparison of viscosity between MD simulation values for Cu-Ar nanofluids.

Under the identical selected temperature of 94.4 K, the error of these data was 0.006% compared to the value of  $2.79 \times 10^{-4} \, \text{Pa} \, \text{s} \, [12]$ . Also, our simulation data were close to the previous experimental value of  $2.80 \times 10^{-4} \, \text{Pa} \, \text{s}$  [38], which demonstrated the stability and availability of the current numerical methods. As shown in Figure 6, the simulated Cu–Ar nanofluids viscosity values rise steadily with increasing volume fraction, which are very close to the simulated values given by Zeroual *et al.* [12], indicating that the established system possesses excellent simulation stability.

#### 4 Results and discussion

# 4.1 Influence of volume fraction and particle type on thermal conductivity

In this section, the impact of the volume fraction of various particles and the influence on the thermal conductivity of nanofluids were investigated systematically. The simulation box used in MD for studying was a cubic box of  $108 \text{ Å} \times 55 \text{ Å} \times 55 \text{ Å}$  in the X, Y, and Z directions containing a single nanoparticle surrounded by the Ar atoms inside the box, due to the heat flow transfer as shown in Figure 1, which was conducted from the leftmost end of the box to the middle, we chose the left half of the box as the total volume of the nanofluids. In Figure 7, the specific four particles based on the actual size of the atoms (1.5% particle volume fraction and diameter of 16.82 Å) are demonstrated in equal scale.

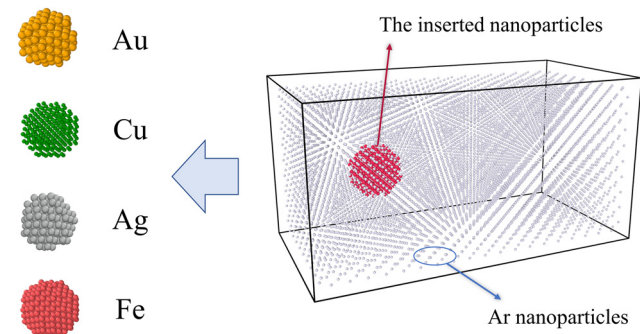


Figure 7: Snapshot of the four particles in nanofluids simulation box.

After calculating the corresponding volume fraction of nanoparticles, spherical atom clusters were filled into the box based on the corresponding radius. After the NVE process, the stability of temperature gradient was observed, and then the temperature difference value corresponding to the most stable temperature gradient was selected and substituted in Eq. (4) for calculation, to obtain the final accurate value of thermal conductivity.

Significantly, an influence of volume fraction on heat conductivity could be observed analytically by the threedimensional smoothed surface plot of Figure 8, which indicates that the heat conductivity of Cu/Au/Ag/Fe-Ar nanofluids increase with the increase in the volume fraction of nanoparticles. For comparison purposes, the relatively varying heat conductivity is admitted, that is, the proportion  $(k_{nf}/k_f)$  between the heat conductivity of the nanofluids  $(k_{nf})$  and base fluids  $(k_f)$  [13]. As can be visualized from the smooth surface in the figure, Ag-Ar nanofluids has the highest average relative thermal conductivity value, followed by Cu-Ar and Au-Ar, while Fe-Ar nanofluids have the lowest value. Ag particles achieve the highest relative thermal conductivity of 1.47 at 2.5% volume fraction, while Fe particles obtain the lowest of 1.02 at 0.5%. In general, the increment of nanoparticle concentration leads to the enhancement of the interfacial effect and is ultimately manifested by the increase in  $k_{\rm nf}/k_{\rm f}$  value with volume fraction [27]. The simulation results in this section further confirm the significant enhancement effect of interfacial layer function for the thermal conductivity [13], as well as in agreement with the previous findings of nanofluids [14,39].

Based on the contours of the bottom surface in the figure, a significant elevation in their relative thermal conductivity values around 1.5% volume fraction is obvious, especially for Cu–Ar nanofluid, while Au–Ar and Fe–Ar nanofluids show relatively flat thermal conductivity with the increase in the volume fraction. The

8 — Ruihao Zhang et al. DE GRUYTER

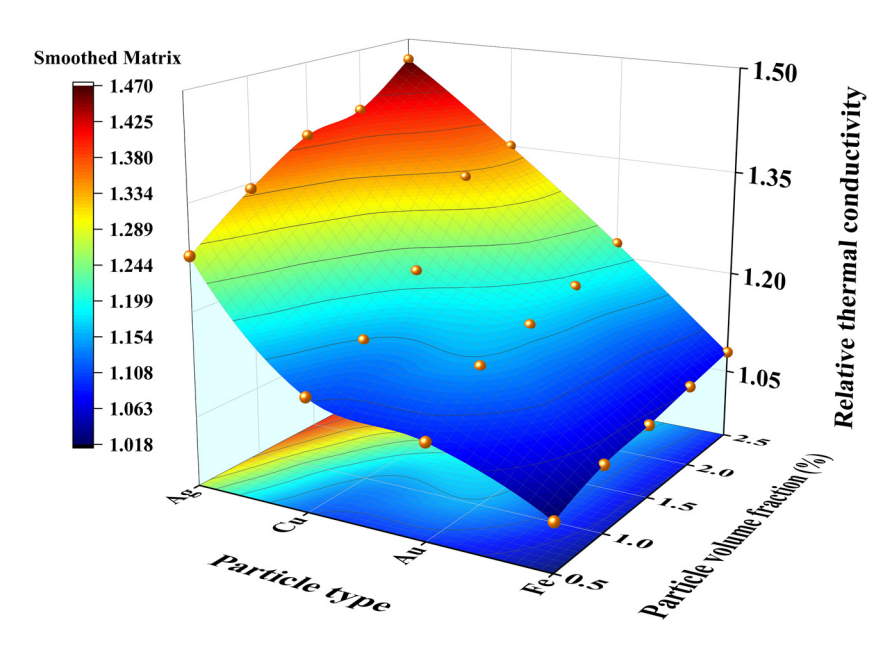


Figure 8: 3D smoothed surface plot of nanofluids volume fraction on thermal conductivity.

fraction with the most significant thermal conductivity properties deserves in-depth research, and the 1.5% volume fraction, which possesses a relatively large improvement in thermal conductivity, provides a good opportunity for this investigation. And it is worthy of a subsequent comprehensive analysis in conjunction with the viscosity performances.

# 4.2 Impact of particle type and volume fraction on viscosity

In this section, the influence of various particle types and volume fractions on the thermal conductivity of nanofluids were investigated systematically, and for this reason, we simulated the viscosity of four different types of nanofluids. The simulation box used in MD for studying was a cubic box of  $55~\text{Å} \times 55~\text{Å} \times 55~\text{Å}$  containing a single nanoparticle surrounded by the Ar atoms. During the NVE calculation, the stability of the velocity gradient was monitored, the most stable velocity gradient was selected, and substituted in Eq. (8) for calculation, with the final viscosity value obtained in the LAMMPS program.

In the absence of simulation work for viscosity comparison of multiple nanofluids, our results compare the viscosity values of nanofluids composed of four particles, respectively. Similarly, the relative viscosity values are used for the convenience of comparing various nanofluids viscosity values, which is the proportion  $(\eta_{nf}/\eta_f)$ 

between the viscosity value of the nanofluids ( $\eta_{nf}$ ) and base fluids ( $\eta_f$ ) [11]. The influence of the nanofluids volume fraction on viscosity is obtained from the 3D smoothed surface plot of Figure 9, which shows that the  $\eta_{nf}/\eta_f$  of Cu/Au/Ag/Fe–Ar nanofluids increase with the increase in the volume fraction of multiple nanoparticles. As can be visualized from the smooth surface in the figure, Au–Ar nanofluids have the highest average relative viscosity value, followed by Ag–Ar and Cu–Ar, while Fe–Ar nanofluids have the lowest value. Au particles achieve the highest relative viscosity of 1.20269 at 2.5% volume fraction, while Fe particles obtain the lowest of 1.00084 at 0.5%.

From the above experimental data, it can be seen that the enhancement of the viscosity of the nanofluids strongly depends on the volume fraction of the nanoparticles, in agreement with the principle of the thermal conductivity enhancement effect, of which the solid-liquid interfacial layer between the liquid and the nanoparticles is considered to be the critical factor [12]. Specifically, since the forces between the nanoparticles and the liquid are much larger than the effects between the atoms of the liquid (as also evident from the L-J potentials in Table 1), a large amount of argon atoms are attracted around the nanoparticles after the formulation of the nanofluids and the adsorption is enhanced as the volume fraction of the particles becomes larger, which leads to the appearance of an ordered liquid layer eventually [40,41]. The analytical demonstration of the improvement of nanofluids viscosity is presented above, followed by a study of the

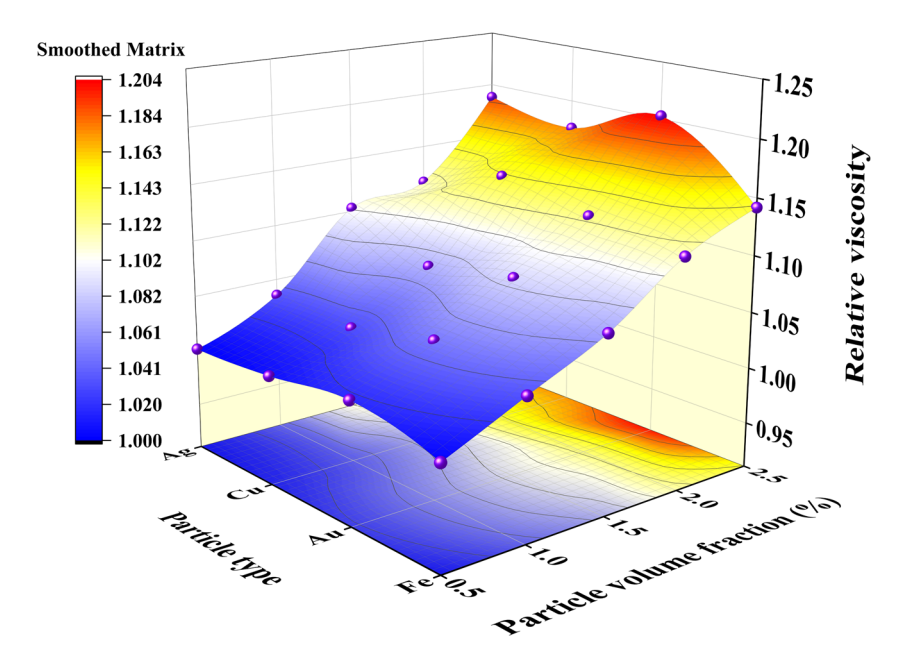


Figure 9: 3D smoothed surface plot of nanofluids volume fraction on viscosity.

microscopic mechanism using the density distribution method.

## 4.3 Number density distribution

In this work, the number density distribution of nanofluids was computed to evaluate the microscopic mechanism of heat transfer and viscosity enhancement, which means density/number is computed for each chunk (number/volume). A better comparison of the density properties of different types of atoms is achieved by dividing the spatially averaged distribution of 20 equally spaced blocks along the *X*-axis in the simulation box. The number of atoms  $\Delta N$  in the chunk spaces  $\Delta V$  can be figured out and used to calculate the number density n, written as follows:

$$n = \frac{\Delta N}{\Delta V}.$$
 (12)

The number density distribution curves of the representative four nanofluids from 0.5 to 2.5% volume fraction under the thermal conductivity simulation conditions are shown in Figure 10, and obviously they have similar characteristics. As the distance along the *X*-axis increases, the curves converge to a steady value, suggesting that the degree of density influenced by the aggregation of nanoparticles decreases with the change in position gradually; while a clear wave peak appear in the vicinity of the spherical center of the metal particles at the beginning of the simulation (sixth bin), indicating

that the argon atoms in the vicinity the nanoparticles are attracted vigorously by the solid interface, which formed the interface nanolayer with great influence. In particular, Au–Ar and Ag–Ar nanofluids behave more or less the same, with the highest value of number density increasing with the volume concentration. The wave range of Cu–Ar nanofluids fluctuate widely, but the starting value of the wave start from the fifth bin basically, and the peak value of 2% volume concentration is around the seventh bin. The performance of Fe–Ar nanofluids is consistent with the wave range concentrated between 2.5th bin and 8.5th bin, and the highest value of number density increases with the volume concentration, showing a linear correlation.

Notably, the position of the mountain peak in the figure denotes the position of the spherical center; the height of the peak reflects the degree of aggregation [28]; and the left and right displacements of the peak indicate the degree of displacement of the spherical particles after the simulation based on the method in this study [42]. As can be seen, the number density distribution is highly related to the atomic masses. For Au and Ag, which have larger atomic masses, the location of the number density peak is relatively fixed, indicating that the atomic clusters do not undergo large vibrations, while for Cu and Fe, which have smaller atomic masses, larger peaks can be observed and there is a larger shift in the position of the peaks as the volume fraction increases. Larger peaks can be observed and the location of the peak has a large shift with the increase in the volume fraction [12].

10 — Ruihao Zhang et al. DE GRUYTER

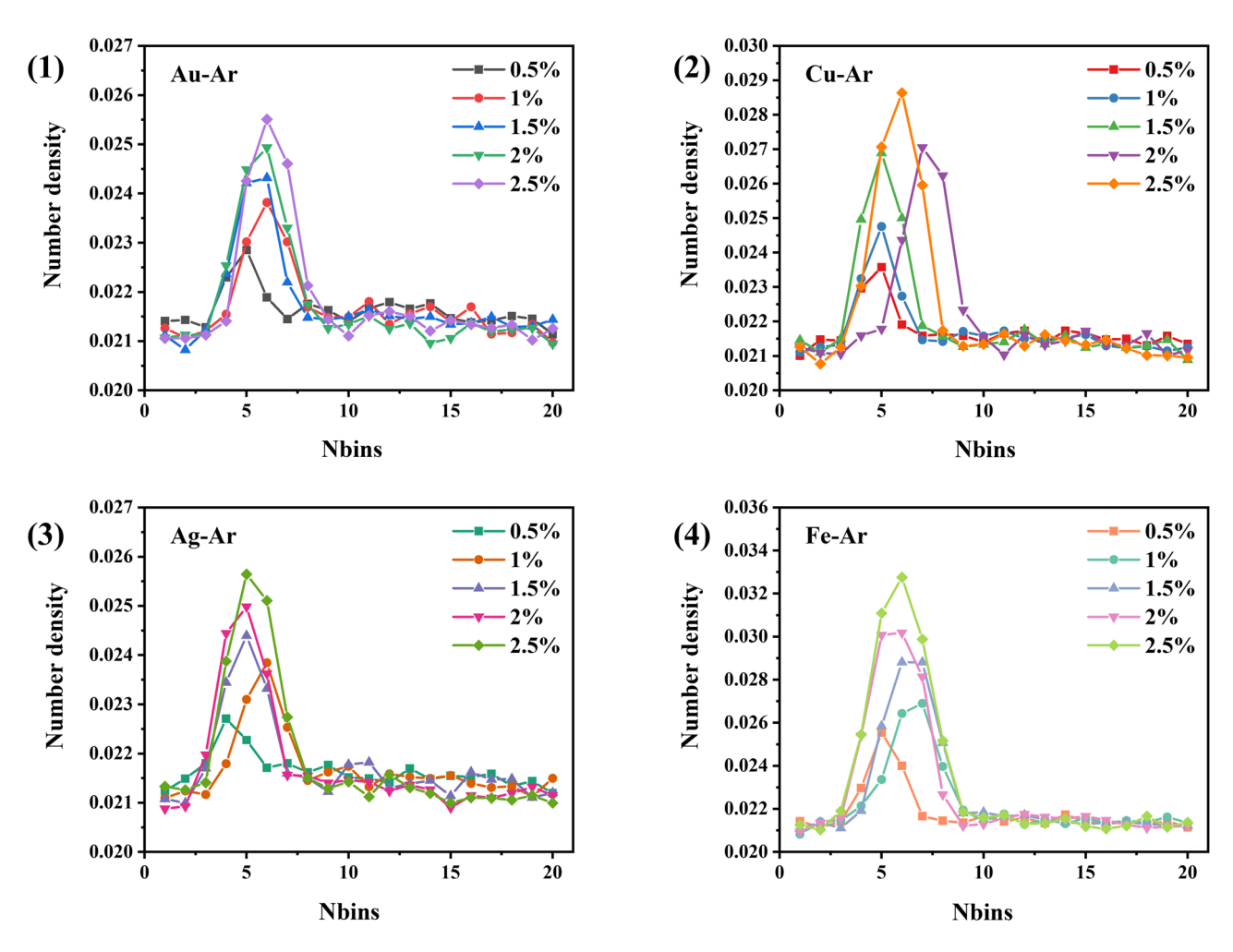


Figure 10: The number density distribution curves of four types of nanofluids from 0.5 to 2.5% volume fraction: (1) Au–Ar, (2) Cu–Ar, (3) Ag–Ar, and (4) Fe–Ar.

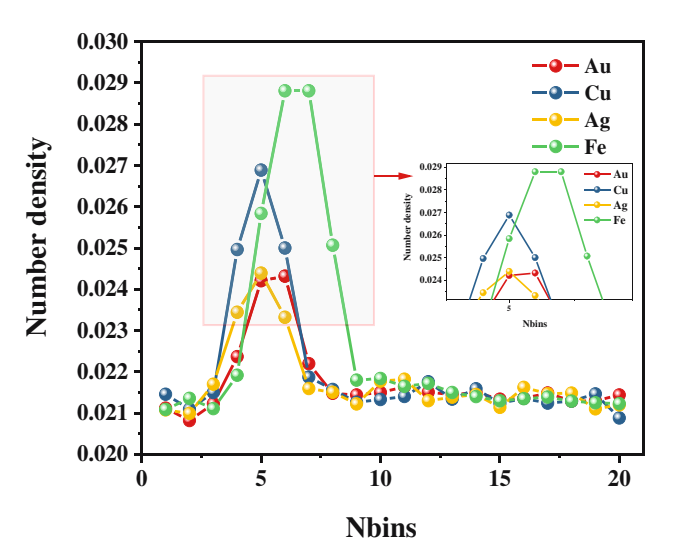


Figure 11: The number density distribution curves of four nanofluids with 1.5% volume fraction.

Figure 11 displays a comparison of the number density distribution curves of four nanofluids with 1.5% volume fraction. Intuitively, the different types of nanofluids possess similar curve characteristics, with distinct peaks near the sixth bin position, followed by the curve returning to a mean density value. As can be seen, the number density distribution correlates highly with the type of particle atoms, with the peak size of Fe > Cu > Ag > Au (0.02881, 0.02689, 0.02439, 0.02432, respectively), which shows positive linear relationship with the atomic mass. In combination with the above analysis, there is a strong correlation between the degree of agglomeration in nanofluid particles and the type of added atoms.

#### 4.4 RDF and MSD

In an attempt to further investigate that how the thermal conductivity and viscosity vary with nanofluids particle

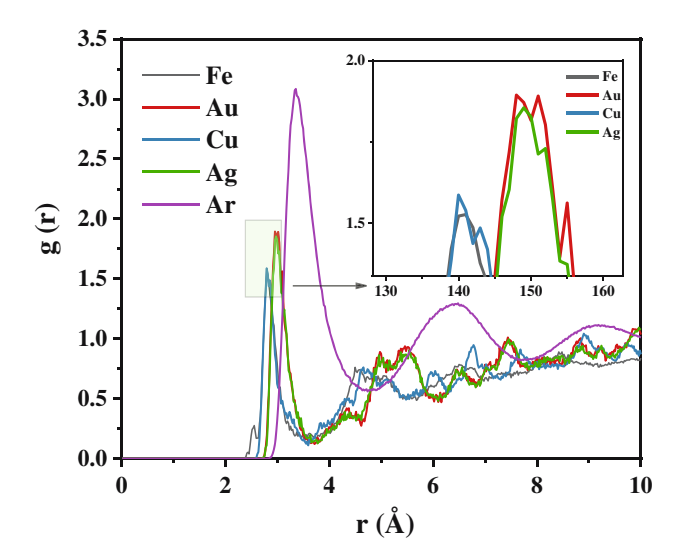


Figure 12: The comparison of RDF curves in different nanofluids.

type and volume fraction, it is important to calculate the RDF and MSD [39]. For this purpose, the MD simulation conditions studied above were used to derive the corresponding data under the thermal conductivity simulation conditions.

The comparative plots of RDF in the nanofluids containing pure Ar and 1.5% volume fraction of metal particles are presented in Figure 12. Intuitively, the deployment of Ar-Ar RDF explains the liquid properties of "short-range order" (observation from the first peak at 4 Å) and "long-range disorder" (observation from the second peak at 7 Å). The first peak position is shifted to the left in the nanofluids compared to the RDF curve of the pure Ar fluid, and the position of the subsequent peaks are distributed evenly, which demonstrates that the microstructure of nanofluids exhibits both "shortrange ordered and long-range disordered" liquid characteristics and "long-range ordered" solid characteristics [43]. The RDF curve exhibits a high and narrow feature in the first peak followed by a broad and flattened feature in the second peak, which further demonstrates that many argon atoms are clustered around the metal particles [36]. The above phenomenon indicates that an even denser nanosphere structure is developed around the nanoparticles. As confirmed by the small detail image, the Au-Ar and Ag-Ar curves match essentially, and all curves are more to the left. The Cu-Ar and Fe-Ar peaks are essentially close to each other, which are consistent with the conclusion of the number density distribution plots for 1.5% particle volume fraction in Figure 11, further indicating the significant effect of different atomic

masses on the interfacial nanolayer. Specifically, the nanolayer around the nanoparticles is recognized as an essential factor to promote thermal conductivity through the presence of interstitial thermal resistance between the liquid and solid states [44], and the main factor for the improvement in thermal conductivity is the increase in density, partly driven by the more organized structure.

Figure 13 shows the specific RDF plots for the four nanofluids, which reveals that the RDF curves vary with the particle volume fraction. The peaks of Au-Ar and Ag-Ar decrease gently with the volume fraction, while the peaks of Cu-Ar and Fe-Ar have a large drop-off and decrease drastically with the addition of volume fraction, which indicates that the aggregation of the nanointerfacial layer does not follow a linear relationship. Combined with the research in this study, it could be inferred that there is a close relationship between the change in RDF peak and the change in thermal conductivity. In addition, besides the positive effect of the nanosphere, the thermal boundary resistance (also known as Kapitza resistance) is considered as an obstacle for enhancing thermal conductivity. To be more specific, owing to the different vibrational properties of the base liquid and the nanoparticles, the phonon scattering occurs at their interface and restricts the heat flow into the nanoparticles resulting in the heat transfer resistance [45]. It is most probably the reason behind the insignificant thermal conductivity enhancement of Fe nanoparticles. In general, the Cu-Ar curve has the most obvious variation, while Au-Ar is the flattest of all, which corresponds with the previous characteristics of thermal conductivity and viscosity completely. Indirectly, it also reflects the better regularity and stability of Au as simulated atom in nanofluids.

To investigate the impact of granular motion on the heat conductivity, we calculated the MSD functions for pure argon and four types of nanofluids under the same simulation conditions. Figure 14 displays the MSD comparison plots for four melt particles with 1.5% volume fraction and the pure Ar at 0–50,000 steps, where the MSD function approximates the straight line increasing with time and the slope of the line is 6D according to Eq. (11).

Therefore, for the purpose of studying the relative movement degree of the four nanoparticles in the nanofluids, the gradients of the lines in Figure 14 were utilized for matching and research. On analyzing the MSD of argon-based fluids, we find that our simulation result (the diffusion coefficient  $D = 2.11 \times 10^{-9}$  m<sup>2</sup>/s) agrees fairly well with the literature values ( $D = 2.10 \times 10^{-9}$  m<sup>2</sup>/s) [19].

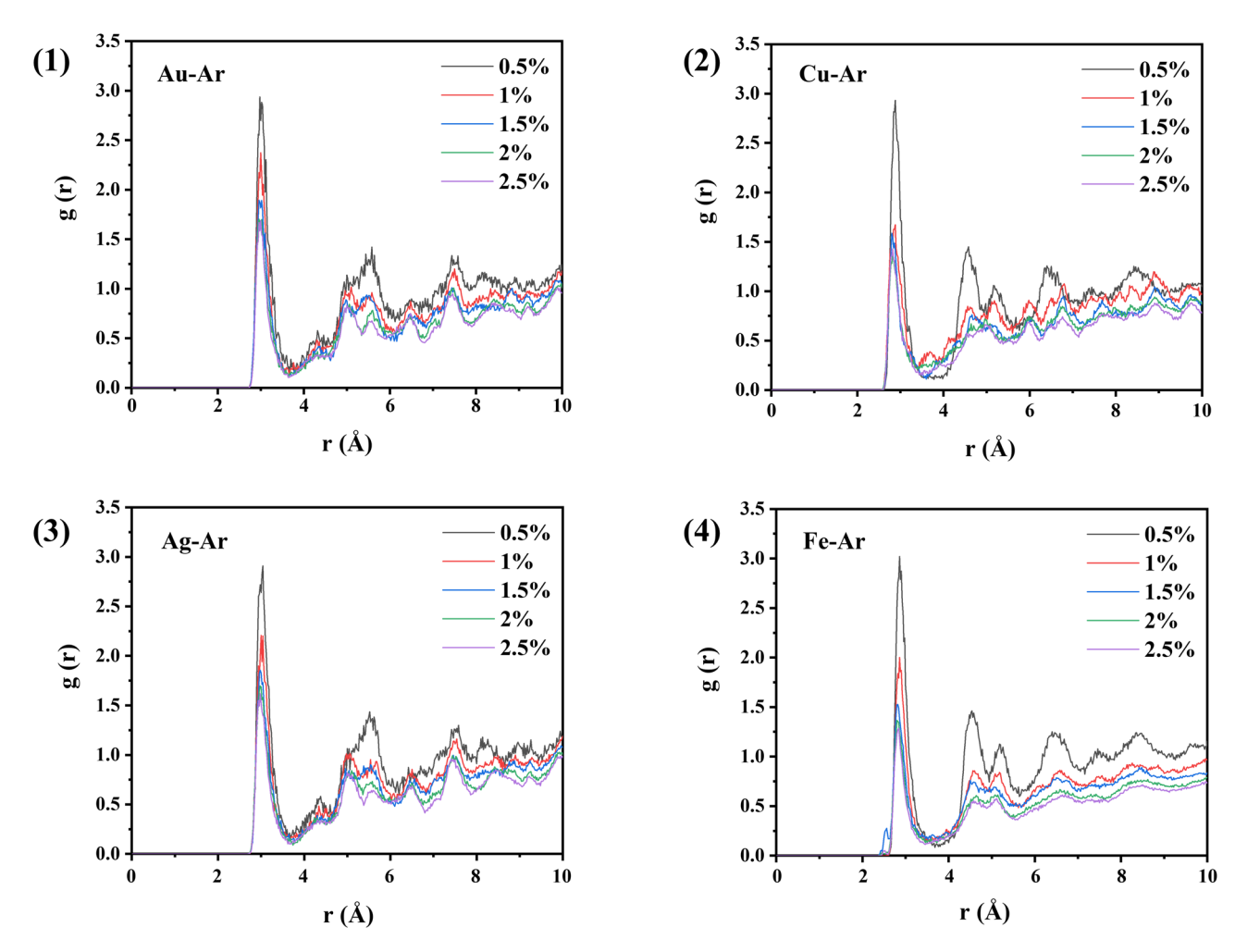


Figure 13: The RDF curves of four types of nanofluids from 0.5 to 2.5% volume fraction: (1) Au-Ar, (2) Cu-Ar, (3) Ag-Ar, and (4) Fe-Ar.

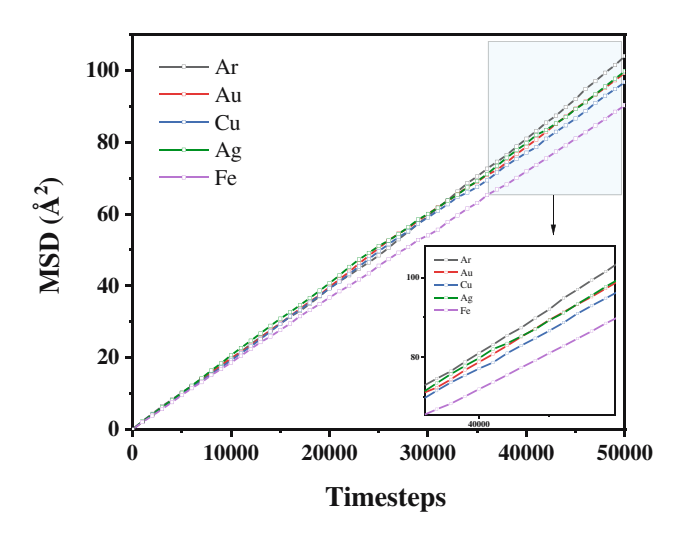


Figure 14: The comparison of MSD profiles in different nanofluids.

The sequences of the lines slopes of the four nanoparticles in the figure show that Ag and Au are almost the same, larger than Cu, and Fe is the smallest, this sequence is also the rank of their diffusion rate in the nanofluids. The gradient of the pure argon fluid line segment is higher than the gradient of the metal particles in the nanofluids suggesting that the diffusion rate of the Ar base fluid will be higher than the nanoparticles, these results correspond to the earlier investigations [8,46]. Collectively, the appearance of the interfacial layer itself provides the foundation for the enhanced thermal conductivity effect [47,48], while the movement of Ar atoms on the interfacial nanosphere is restricted by the nanoparticles, further enhancing the resistance to fluid slippage and leading to an increase in nanofluids viscosity ultimately.

## 5 Conclusion

**DE GRUYTER** 

Throughout the study, the influences of different nanoparticles properties on thermal conductivity and viscosity of the nanofluids were investigated, and NEMD and RNEMD calculations were employed to research the impacts of nanoparticle type and volume fraction on the performances of nanofluids. The Au-Ar and Ag-Ar nanofluids showed the largest relative thermal conductivity and viscosity under the same condition comparison, and exhibited superior stability in number density distribution than Cu-Ar and Fe-Ar nanofluids. The combined experimental data suggest that the viscosity enhancement corresponds to the principle of the thermal conductivity strengthening effects, where the solid-liquid interfacial layer between the liquid and the nanoparticles considered to be the key factor. The simulation results showed that Au nanoparticle performed with excellent stability and regularity in RDF and MSD, which was the expected candidate for nanofluids simulation.

Funding information: Financial support from National Natural Science Foundation of China under Contract (No. 51966005 and No. 52069010); Yunnan Fundamental Research Projects (No. 202101AT070120 and No. 202301AT 070469); Yunnan Major Scientific and Technological Projects (No. 202202AG050002) are gratefully acknowledged.

Author contributions: All authors have accepted responsibility for the entire content of this manuscript and approved its submission.

Conflict of interest: The authors state no conflict of interest.

#### References

- Narankhishig Z, Ham J, Lee H, Cho H. Convective heat transfer characteristics of nanofluids including the magnetic effect on heat transfer enhancement - a review. Appl Therm Eng. 2021;193:116987.
- Qiu L, Zhu N, Feng Y, Michaelides EE, Żyła G, Jing D, et al. A review of recent advances in thermophysical properties at the nanoscale: From solid state to colloids. Phys Rep. 2020;843:1-81.
- Das SK, Choi SUS, Patel HE. Heat transfer in nanofluids A review. Heat Transf Eng. 2006;27:3-19.
- Saidur R, Leong KY, Mohammad HA. A review on applications and challenges of nanofluids. Renew Sustain Energy Rev. 2011;15:1646-68.

- Li Y, Zhai Y, Ma M, Xuan Z, Wang H. Using molecular dynamics simulations to investigate the effect of the interfacial nanolayer structure on enhancing the viscosity and thermal conductivity of nanofluids. Int Commun Heat Mass Transf. 2021;122:105181.
- Bhanushali S, Jason NN, Ghosh P, Ganesh A, Simon GP, Cheng W. Enhanced thermal conductivity of copper nanofluids: the effect of filler geometry. ACS Applied Materials & Interfaces. 2017;9(22):18925-35.
- [7] Ghosh MM, Ghosh S, Pabi SK. Effects of particle shape and fluid temperature on heat-transfer characteristics of nanofluids. J Mater Eng Perform. 2013;22:1525-9.
- Zhou L, Zhu J, Zhao Y, Ma H. A molecular dynamics study on thermal conductivity enhancement mechanism of nanofluids -Effect of nanoparticle aggregation. Int J Heat Mass Transf. 2022;183:122124.
- [9] Liao J, Zhang A, Qing S, Zhang X, Luo Z. Investigation on the aggregation structure of nanoparticle on the thermal conductivity of nanofluids by molecular dynamic simulations. Powder Technol. 2022;395:584-91.
- [10] Lou Z, Yang M. Molecular dynamics simulations on the shear viscosity of Al<sub>2</sub>O<sub>3</sub> nanofluids. Comput Fluids. 2015;117:17-23.
- Jabbari F, Rajabpour A, Saedodin S. Viscosity of carbon [11] nanotube/water nanofluid: Equilibrium molecular dynamics. J Therm Anal Calorim. 2019;135:1787-96.
- Zeroual S, Loulijat H, Achehal E, Estellé P, Hasnaoui A, Ouaskit S. Viscosity of Ar-Cu nanofluids by molecular dynamics simulations: Effects of nanoparticle content, temperature and potential interaction. J Mol Liq. 2018;268:490-6.
- Essajai R, Mzerd A, Hassanain N, Qjani M. Thermal conductivity enhancement of nanofluids composed of rod-shaped gold nanoparticles: Insights from molecular dynamics. J Mol Liq. 2019;293:111494.
- [14] Essajai R, Rachadi A, Feddi E. MD simulation-based study on the thermodynamic, structural and liquid properties of gold nanostructures. Mater Chem Phys. 2018;218:116-21.
- [15] Milanese M, Iacobazzi F, Colangelo G, Risi. AD. An investigation of layering phenomenon at the liquid-solid interface in Cu and CuO based nanofluids. Int J Heat Mass Transf. 2016:103:564-71.
- [16] Akiner T, Kocer E, Mason JK, Erturk H. Green-Kubo assessments of thermal transport in nanocolloids based on interfacial effects . Mater Today Commun. 2019;20:100533.
- [17] Guo H, Zhao N. Interfacial layer simulation and effect on Cu-Ar nanofluids thermal conductivity using molecular dynamics method. J Mol Liq. 2018;259:40-7.
- [18] Cui W, Shen Z, Yang J, Wu S, Bai M. Influence of nanoparticle properties on the thermal conductivity of nanofluids by molecular dynamics simulation. RSC Adv. 2014;4:55580-9.
- Cui W, Shen Z, Yang J, Wu S. Molecular dynamics simulation on the microstructure of absorption layer at the liquid-solid interface in nanofluids. Int Commun Heat Mass Transf. 2016:71:75-85.
- [20] Wang X, Jing D. Determination of thermal conductivity of interfacial layer in nanofluids by equilibrium molecular dynamics simulation. Int J Heat Mass Transf. 2019;128:199-207.
- [21] Thompson AP, Aktulga HM, Berger R, Bolintineanu DS, Brown WM, Crozier PS, et al. Plimpton, LAMMPS - a flexible

- simulation tool for particle-based materials modeling at the atomic, meso, and continuum scales. Comput Phys Commun. 2022;271:108171.
- [22] Nguyen TD. GPU-accelerated Tersoff potentials for massively parallel molecular dynamics simulations. Comput Phys Commun. 2017;212:113-22.
- [23] Stukowski A. Visualization and analysis of atomistic simulation data with OVITO-the Open Visualization Tool. Model Simul Mater Sci Eng. 2009;18:015012.
- [24] Zoli L, Sciti D, Sani E. Zirconium diboride-based nanofluids for solar energy applications. J Mol Liq. 2021;322:114981.
- [25] Daw MS, Baskes MI. Embedded-atom method: Derivation and application to impurities, surfaces, and other defects in metals. Phys Rev B Condens Matter. 1984;29:6443–53.
- [26] Topal I, Servantie J. Molecular dynamics study of the thermal conductivity in nanofluids. Chem Phys. 2019;516:147-51.
- [27] Fujiwara K, Daimo M, Ueki Y, Ohara T, Shibahara M. Thermal conductivity of nanofluids: A comparison of EMD and NEMD calculations. Int J Heat Mass Transf. 2019;144:118695.
- [28] Zhang L, Tian L, Jing Y, Qu P, Zhang A. Molecular dynamics study on the mechanism of nanofluid coolant's thermal conductivity improvement. J Mol Liq. 2022;345:118228.
- [29] Ikeshoji T, Hafskjold B. Non-equilibrium molecular dynamics calculation of heat conduction in liquid and through liquid-gas interface. Mol Phys. 1994;81:251–61.
- [30] Fernandez GA, Vrabec J, Hasse H. A molecular simulation study of shear and bulk viscosity and thermal conductivity of simple real fluids. Fluid Phase Equilib. 2009;221:157-63.
- [31] Müller-Plathe F. Reversing the perturbation in non-equilibrium molecular dynamics: An easy way to calculate the shear viscosity of fluids. Phys Rev E. 1999;59:4894–8.
- [32] Rostami S, Zarringhalam M, Alizadeh A, Toghraie D, Shahsavar A. Goldanlou, molecular dynamic simulation of argon boiling flow inside smooth and rough microchannels by considering the effects of cubic barriers. J Mol Liq. 2020;312:113130.
- [33] Kanhaiya K, Kim S, Im W, Heinz H. Accurate simulation of surfaces and interfaces of ten FCC metals and steel using Lennard-Jones potentials. Npj Comput Mater. 2021;7:17.
- [34] Shibuta Y, Suzuki T. A molecular dynamics study of cooling rate during solidification of metal nanoparticles. Chem Phys Lett. 2011;502:82-6.
- [35] Sarkar S, Selvam RP. Molecular dynamics simulation of effective thermal conductivity and study of enhanced thermal transport mechanism in nanofluids. J Appl Phys. 2007;102:280.

- [36] Chen J, Han K, Wang S, Liu X, Wang P, Chen J. Investigation of enhanced thermal properties of CuAr nanofluids by reverse non equilibrium molecular dynamics method. Powder Technol. 2019;356:559–65.
- [37] Wang R, Qian S, Zhang Z. Investigation of the aggregation morphology of nanoparticle on the thermal conductivity of nanofluid by molecular dynamics simulations. Int J Heat Mass Transf. 2018;127:1138–46.
- [38] Song HL, Dong KP, Kang DB. Molecular dynamics simulations for transport coefficients of liquid argon: new approaches. Bulletin of the Korean Chemical Society. 2003;24(2).
- [39] Essajai R, Tabtab I, Mzerd A, Mounkachi O, Hassanain N, Qjani M. Molecular dynamics study of thermal properties of nanofluids composed of one-dimensional (1-D) network of interconnected gold nanoparticles. Results Phys. 2019;15:102576.
- [40] Garg J, Poudel B, Chiesa M, Gordon J, Ma J, Wang J, et al. Enhanced thermal conductivity and viscosity of copper nanoparticles in ethylene glycol nanofluid. J Appl Phys. 2008;103:074301.
- [41] Kole M, Dey TK. Enhanced thermophysical properties of copper nanoparticles dispersed in gear oil. Appl Therm Eng. 2013:56:45-53.
- [42] Wu N, Zeng L, Fu T, Wang Z, Lu C. Molecular dynamics study of rapid boiling of thin liquid water film on smooth copper surface under different wettability conditions. Int J Heat Mass Transf. 2020;147:118905.
- [43] Wang X, Jing D. Determination of thermal conductivity of interfacial layer in nanofluids by equilibrium molecular dynamics simulation. Int J Heat Mass Transf. 2019;128:199-207.
- [44] Liang Z, Tsai HL. Thermal conductivity of interfacial layers in nanofluids. Phys Rev E. 2011;83:041602.
- [45] Nejatolahi M, Golneshan AA, Kamali R, Sabbaghi S. Nonequilibrium versus equilibrium molecular dynamics for calculating the thermal conductivity of nanofluids. J Therm Anal Calorim. 2021;144:1467–81.
- [46] Li Z, Cui L, Li B, Du X. Enhanced heat conduction in molten salt containing nanoparticles: Insights from molecular dynamics. Int J Heat Mass Transf. 2020;153:119578.
- [47] Pryazhnikov MI, Minakov AV, Rudyak VY, Guzei DV. Thermal conductivity measurements of nanofluids. Int J Heat Mass Transf. 2017;104:1275–82.
- [48] Shi W, Li F, Lin Q. Effects of nanoparticles on the instability of liquid jets in a gaseous crossflow. Int J Multiph Flow. 2020;133:103449.